PHYSICAL REVIEW LETTERS

Measurements of the MHD Dynamo in the Quasi-Single-Helicity Reversed-Field Pinch

P. Piovesan,[1] D. Craig,[2] L. Marrelli,[1] S. Cappello,[1] and P. Martin[1,3]

[1]*Consorzio RFX, Associazione EURATOM-ENEA sulla Fusione, Corso Stati Uniti,4 35127 Padova, Italy*
[2]*Department of Physics, University of Wisconsin, 1150 University Avenue, Madison, Wisconsin 53706, USA*
[3]*Department of Physics, University of Padova, Padova, Italy*

The first experimental study of the MHD dynamo in a quasi-single-helicity (QSH) reversed-field pinch toroidal plasma is presented. In QSH plasmas, a dominant wave number appears in the velocity fluctuation spectrum. This velocity component extends throughout the plasma volume and couples with magnetic fluctuations to produce a significant MHD dynamo electric field. The narrowing of the velocity fluctuation spectrum and the single-mode character of the dynamo are features predicted by theory and computation, but only now are observed in experiment.

The persistence of strong magnetic fields for periods much longer than the resistive diffusion time in a variety of natural and laboratory systems is thought to be due to dynamo mechanisms, which in large part rely on MHD turbulence and related self-organization processes [1]. The basic mechanisms which are responsible for dynamos are not yet completely known, often due to a lack of precise and direct measurements. A strong effort has thus been made to study MHD turbulence and dynamos in well-diagnosed laboratory experiments [2,3]. Dynamo effects beyond single fluid MHD (e.g., the two-fluid Hall dynamo) have also been studied recently both experimentally and theoretically [4]. The reversed-field pinch (RFP) is a device for the confinement of toroidal plasmas, which offers a good opportunity to study basic dynamo mechanisms by means of advanced diagnostics and 3D nonlinear MHD codes [5,6]. The RFP toroidal magnetic field with its characteristic reversal is sustained in time by a dynamo, which relies on the spontaneous excitation of magnetic modes with poloidal mode number $m = 0, 1$ and various toroidal mode numbers n [3–8]. Plasma self-organization produces the right amount of dynamo electric field, $\mathbf{E}_d$, to satisfy the mean field Ohm's law, $\mathbf{E}_0 + \mathbf{E}_d = \eta\mathbf{J}_0$. Here $\mathbf{J}_0$ is the current density, $\mathbf{E}_0$ is the externally applied toroidal electric field, and η the plasma resistivity. Lacking $\mathbf{E}_d$, $\mathbf{E}_0$ could not drive the current density profile $\mathbf{J}_0$ needed to produce the RFP magnetic configuration. In particular both in experiments and numerical simulations $\mathbf{E}_d$ tends to suppress toroidal current in the core and to drive poloidal current at the edge [3,5,9].

In the standard multiple helicity (MH) conditions, the dynamo instabilities have a wide n spectrum and induce magnetic chaos over large portions of the plasma [3,5]. This magnetic chaos limits confinement [10,11]. Theory predicts that a laminar regime called single helicity (SH) can be achieved through a spontaneous transition [12]. Magnetic field generation in SH does not rely on broadband turbulence but on a laminar process. A SH RFP is a helical Ohmic equilibrium with good confinement prop-

erties, and could be very appealing for fusion. The symmetry breaking necessary for dynamo is provided by a global helical deformation of the magnetic flux surfaces produced by a single saturated resistive kink mode [13]. This helical kink mode is driven by a global plasma flow dominated by an $m = 0$ pinch term and by an $m = 1$ component of comparable amplitude. Figure 1 reports the $m = 1$ component of this flow velocity vector field projected onto a poloidal cross section of the torus, obtained with SpeCyl [9], a 3D nonlinear viscoresistive MHD code with cylindrical geometry. The interaction between the $m = 1$ magnetic and velocity fields is responsible for mean field dynamo generation in numerical SH plasmas.

SH has not been experimentally achieved, but a partial transition to a helical state called quasisingle helicity (QSH) has been observed [14,15]. In QSH, opposite to the broad MH spectrum of instabilities, one mode with $m = 1$ and $n = n_0$ dominates over all others in the magnetic field spectrum. As a result nested helical isoemissive flux surfaces with good confinement properties are observed in experiments [14], though magnetic stochasticity still exists outside these structures. QSH regimes are predicted by theory to exist in the transition region
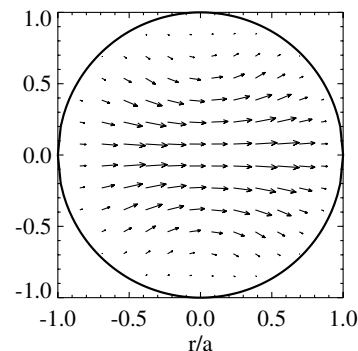

FIG. 1. Projection of the $m = 1$ component of the flow velocity vector field onto the poloidal cross section of the torus for an SH state from the SpeCyl MHD code.

between MH and SH [12]. Thus, despite its lack of purity in comparison with SH, QSH is regarded as a significant step towards the experimental realization of a helical RFP.

While the structure of the dynamo electric field $\mathbf{E}_d$ in MH conditions has been studied both experimentally [3,7,8] and numerically [5,9,16,17], very little is known about $\mathbf{E}_d$ in QSH. In particular, two important questions are still open, which are stimulated by the aforementioned numerical results: (i) Is there in QSH a global plasma flow pattern with the same geometrical helicity as the dominant magnetic mode? and (ii) Is this dominant instability producing any dynamo?

In this Letter we present the first experimental study of the MHD dynamo in a QSH RFP. Data have been taken in the Madison Symmetric Torus (MST) experiment (major radius $R_0 = 1.5$ m, minor radius $a = 0.52$ m) [18]. It will be first shown that during QSH periods a global helical flow pattern appears with the same helicity as the dominant magnetic mode ($m = 1$, $n = 6$). This is rather different from what is observed in standard turbulent MH plasmas. The $\tilde{\mathbf{v}}^{(1,6)}$ velocity perturbation couples to the corresponding magnetic mode $\tilde{\mathbf{b}}^{(1,6)}$, so as to generate a finite axisymmetric dynamo electric field $\mathbf{E}_d^{(1,6)} = \langle \tilde{\mathbf{v}}^{(1,6)} \times \tilde{\mathbf{b}}^{(1,6)} \rangle$. We will show direct measurements of its toroidal component $E_{d,\phi}^{(1,6)}$. Almost all of the measured dynamo electric field in QSH is produced by the dominant mode and is consistent with that required to sustain the RFP configuration as predicted by SpeCyl.

Our analysis proceeds as follows: (i) measurement of flow velocity fluctuations, (ii) correlation of the velocity signals with magnetic mode amplitudes $\tilde{\mathbf{b}}^{(1,n)}$ and derivation of the velocity $(1, n)$ spatial spectrum, (iii) comparison of the experimental results with SpeCyl and (iv) computation of the toroidal dynamo electric field $E_{d,\phi}^{(1,n)}$.

The magnetic fluctuation spectrum is measured by a toroidal array of 32 coils. The equilibrium and fluctuating ion flow velocities are measured by the Ion Dynamics Spectrometer (IDS) [19]. The IDS collects CV line radiation ($\lambda = 227.1$ nm) from intrinsic impurity ions along six parallel chords in the same poloidal cross section almost perpendicular to the equatorial plane. It has been shown before in MST [20] that the ion flow velocity is well measured by the Doppler shift of the CV line. The IDS velocity measured by a chord with unit vector $\vec{\ell}$ is the line average of the flow velocity vector field $\vec{\mathbf{v}}$ projected along the chord, locally weighted by the CV line emissivity I_{CV}:

$$v_L = \frac{\int_L \vec{\mathbf{v}} \cdot \vec{\ell} I_{CV} dL}{\int_L I_{CV} dL}. \qquad (1)$$

For a uniform I_{CV} profile, the v_L signal measured by central chords would be dominated by the radial component $\tilde{v}_r$ of the $m = 1$ fluctuating velocity field, while off-

axis chords would be dominated by the poloidal component $\tilde{v}_\theta$. The MST plasmas examined here have a hollow CV emissivity profile and hence $\tilde{v}_\theta$ dominates for all chords. To obtain the $(1, n)$ spatial spectrum of the velocity fluctuations, the single chord velocity measurement v_L is correlated with each $(1, n)$ magnetic mode amplitude. From standard Fourier analysis of the 32 coil signals we obtain the amplitude $\tilde{b}^{(1,n)}(t)$ and phase $\varphi_b^{(1,n)}(t)$ of each magnetic mode as a function of time. As each mode rotates, the spatially coherent part of the flow velocity also rotates, giving rise to time oscillations in the $v_L(t)$ time series at the poloidal rotation frequencies $(2\pi)^{-1} d\varphi_b^{(1,n)}/dt$ [7]. Therefore the amplitude of the mode resolved flow velocity fluctuations $\tilde{v}_L^{(1,n)}$ can be computed as

$$\tilde{v}_L^{(1,n)} = \sqrt{2 \int_0^{f_{max}} df P_v(f) \gamma_{vb}^{(1,n)2}(f)}, \qquad (2)$$

where $P_v(f)$ is the auto-power spectrum of the velocity time series $v_L(t)$, $\gamma_{vb}^{(1,n)}(f)$ is the coherence function between $v_L(t)$ and the $(1, n)$ magnetic mode amplitude $\tilde{b}_\theta^{(1,n)}(t) \cos[\varphi_b^{(1,n)}(t)]$ measured at the plasma edge. $f_{max} = 50$ kHz is the diagnostic bandwidth. Although $\tilde{b}_\theta^{(1,n)}$ is measured at the edge, both theory [5,9] and experiment [21,22] have confirmed that the magnetic modes are global in character, and hence $\tilde{b}^{(1,n)}$ in the core can be reliably estimated from $\tilde{b}_\theta^{(1,n)}$ at the edge.

The coherence functions and the autopower spectra are estimated statistically [23]. A database of 580 similar discharges has been analyzed to retrieve QSH and MH periods. All discharges are characterized by a plasma current $I_p \approx 300$ kA, electron density $n_e \approx 1 \times 10^{19}$ m^{-3} and reversal parameter $F = B_\phi(a)/\langle B_\phi \rangle \approx -0.2$ (here B_ϕ is the toroidal magnetic field). It has been shown in [15] that these MST plasmas have a finite probability ($\approx 25\%$) of accessing a QSH state from an initial MH regime. A code thus searches the whole database of discharges for MH and QSH periods. As in [14,15], the search criterion is based on the spectral index N_S, defined as $N_S = [\sum_n (W_n / \sum_{n'} W_{n'})^2]^{-1}$, where W_n is the magnetic energy of the $(1, n)$ mode. A pure SH spectrum corresponds to $N_S = 1$ and we have chosen that $N_S < 2$ defines a QSH state, while $N_S > 3$ defines MH. QSH and MH periods are selected only between sawteeth, which are discrete dynamo events, during which a burst in the magnetic and flow velocity fluctuation amplitude is recorded and toroidal magnetic flux is suddenly amplified [7]. Each QSH (or MH) period found by the code is divided into 0.5 ms long subperiods and two ensembles of similar events, the QSH and MH ensembles, are built up. Only periods with rotating modes are included in the two ensembles. The mode analysis of magnetic and flow velocity fluctuation signals is applied to

each QSH (or MH) event. An average of all events is then performed over the QSH (or MH) ensemble, respectively.

In Fig. 2 the ensemble-averaged spatial toroidal spectra for $m = 1$ modes are reported both for the magnetic $\tilde{b}_\theta^{(1,n)}$ and the flow velocity $\tilde{v}_L^{(1,n)}$ fluctuation amplitude. Error bars in Fig. 2 represent the width of the $\tilde{b}_\theta^{(1,n)}$ and $\tilde{v}_L^{(1,n)}$ sampling distribution as derived by propagation of standard errors of autopower spectra and coherence functions [23]. As noted in the past, the magnetic $(1, n)$ spectrum is peaked around the dominant $(1, 6)$ mode during QSH states, while it is rather broad during MH [14,15] [see Figs. 2(a) and 2(b)]. The present measurements show that, also in the flow velocity spectrum, the $(1, 6)$ mode clearly emerges over the other modes during QSH [see Figs. 2(c) and 2(d)]. No dominant mode is present in MH. This constitutes the first proof that during QSH the same dominant wave number as in the magnetic fluctuation appears in the velocity fluctuation spectrum, so that an ordered helical flow pattern emerges when the plasma approaches a helical state.

In Fig. 3 the velocity fluctuation amplitude is reported as a function of the normalized impact parameter p/a of the six IDS chords. The profile of the $\tilde{v}_L^{(1,6)}$ amplitude in QSH (continuous line) is compared with those of the average amplitude of the secondary modes ($n = 7$–12) in QSH (dashed line) and of all modes ($n = 6$–12) in MH (dotted line). The $(1, 6)$ mode is larger than the other n's throughout the entire plasma. The average secondary mode amplitude is equal for QSH and MH within error bars. The $\tilde{v}_L^{(1,6)}$ profile is hollow due to the hollow CV emission profile and there is also a slight asymmetry due possibly to toroidal effects.

More detailed information on the local flows are obtained by fitting the experimental profiles with model flows. We constrain the form of the model flow, by examining the flow pattern of a QSH state predicted by SpeCyl (Lundquist number $S = 10^5$, dominant helicity $n_0 = 10$

and aspect ratio $R_0/a = 4$). The $(1, n_0)$ component of the numerical QSH velocity vector field can be described by $\tilde{\mathbf{v}}^{(1,n_0)}(r, \theta, \phi) = \tilde{v}_r^{(1,n_0)}(r)\cos(\theta - n_0\phi)\hat{\mathbf{r}} + \tilde{v}_\theta^{(1,n_0)}(r)\cos(\theta - n_0\phi + \pi/2)\hat{\theta}$, where $\tilde{v}_r^{(1,n_0)}$ and $\tilde{v}_\theta^{(1,n_0)}$ are positive amplitude functions. Experimental data are well fit by the radial functions $\tilde{v}_r^{(1,n_0)} = (1 - r^2)^6$ and $\tilde{v}_\theta^{(1,n_0)} = (1 - r^2)^{2.5}$. Assuming that the velocity pattern is rigidly rotating in the toroidal direction and using the measured CV emissivity profile, time fluctuations in the IDS line averages for the model flow can be computed. In Fig. 4(a) we show the modeled (continuous line) and experimental (symbols) fluctuation amplitude profiles for the dominant mode as a function of the chord impact parameter p/a. Figure 4(b) shows the projection of the velocity vector field thus obtained onto the poloidal cross section, whose central part closely resembles that of Fig. 1. The measured flow fluctuation $\tilde{v}_L$ is mostly due to the poloidal component of the field, since the fitted radial function $\tilde{v}_r^{(1,n_0)}(r)$ is rather concentrated in the plasma core where the CV emissivity is small.

The toroidal component of the flux surface averaged dynamo electric field $E_{d,\phi}$ has been estimated, in a way similar to [7]. The poloidal component of $\mathbf{E}_d$ cannot be measured with the available viewing geometry. Over a complete cycle of poloidal rotation, the IDS lines of sight sample the whole flux surface: therefore time averages are a good approximation of spatial averages. In particular, the toroidal component of the dynamo electric field generated by the $(1, n)$ mode is given by

$$E_{d,\phi}^{(1,n)} = \langle \tilde{\mathbf{v}}^{(1,n)} \times \tilde{\mathbf{b}}^{(1,n)} \rangle_\phi \approx \frac{1}{2} \tilde{v}_\theta^{(1,n)} \tilde{b}_r^{(1,n)} \cos\Phi_{vb}^{(1,n)}, \quad (3)$$

where we have neglected the $\tilde{v}_r^{(1,n)} \tilde{b}_\theta^{(1,n)}$ term, since $\tilde{v}_r^{(1,n)}$ contributes little to the IDS measurements, as previously discussed. In Eq. (3), $\Phi_{vb}^{(1,n)}$ represents the phase delay between the radial magnetic field $\tilde{b}_r^{(1,n)}$ and $\tilde{v}_\theta^{(1,n)}$. We
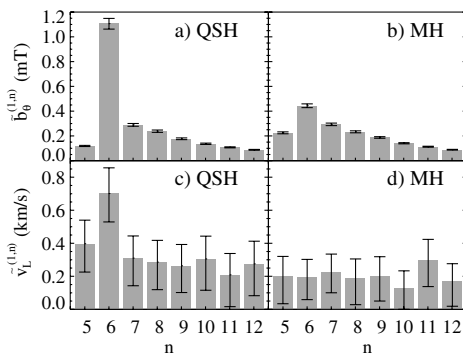
FIG. 2. The $(m = 1, n)$ spectra averaged over the QSH and MH ensembles for the magnetic [(a),(b)] and the flow velocity [(c),(d)] dynamo modes from a chord with impact parameter $p/a = -0.34$. The error bars represent the standard deviation of the mean.
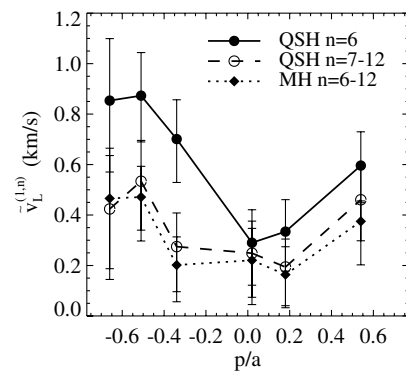
FIG. 3. The flow velocity mode amplitude vs the impact parameter for the dominant $(1, 6)$ mode in QSH (full circles, continuous line), the average of secondary modes ($n = 7$–12) in QSH (empty circles, dashed line) and of all modes ($n = 6$–12) in MH (diamonds, dotted line).
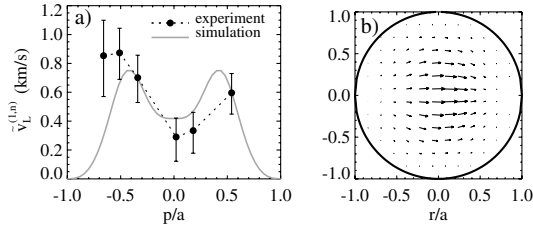
FIG. 4.   (a) Comparison between the experimental $\tilde{v}_L^{(1,6)}$ dominant mode amplitude in QSH (dots) and the modeled data based on QSH runs of the SpeCyl code (continuous line). (b) Projection of the modeled $m = 1$ flow velocity vector field onto the poloidal cross section.
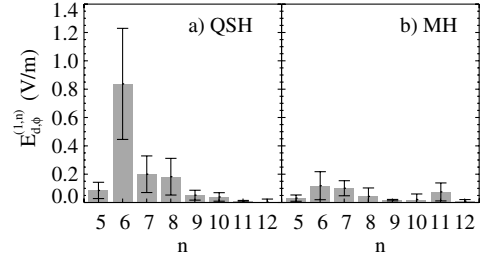

FIG. 5.   The contribution $E_{d,\phi}^{(1,n)}$ of different $(m = 1, n)$ modes to the toroidal dynamo electric field averaged over the QSH (a) and MH (b) ensembles.

determine $E_{d,\phi}^{(1,n)}$ by evaluating the cross power-spectrum $P_{vb}(f)$ between the flow fluctuations and the time series of the $(1, n)$ magnetic mode amplitudes. $\Phi_{vb}^{(1,n)}$ is given by $\Phi_{vb}^{(1,n)}(f) = \arg P_{vb}^{(1,n)}(f)$, and $E_{d,\phi}^{(1,n)}$ can be obtained by integration over frequency

$$E_{d,\phi}^{(1,n)} = \int_0^{f_{\max}} df |P_{vb}^{(1,n)}(f)| \cos[\Phi_{vb}^{(1,n)}(f)]. \qquad (4)$$

Figure 5 shows the contribution from each $(1, n)$ mode to $E_{d,\phi}$, averaged over the QSH [Fig. 5(a)] and the MH [Fig. 5(b)] ensembles. The error bars represent the standard deviation of the mean. In this case the IDS chord with impact parameter $p/a = -0.34$ has been used, but similar results are found for other chords. The sign of $E_{d,\phi}^{(1,6)}$ is positive. In the reference frame used here, a positive toroidal component of $\mathbf{E}_d$ has a sign opposite to that of the applied inductive electric field, i.e., tends to suppress toroidal electric current. This is consistent with numerical simulations in this region of the plasma [5]. The dominant $(1, 6)$ mode produces a flux surface averaged QSH electric field $E_{d,\phi}^{(1,6)} \sim 1$–2 V/m, as shown also by other chords. This is consistent in magnitude with that needed to sustain the magnetic configuration in time. It is in fact a significant fraction of the inductively driven electric field ($\simeq 2$ V/m) in these discharges. The behavior of the dynamo electric field in QSH plasmas is therefore different from that in MH. In MH previous measurements have shown that $\mathbf{E}_d$ is primarily generated in discrete events [7,8]. The MHD dynamo in these cases is inherently transient and turbulent in nature: a sudden ($\delta t \simeq 100$ μs) and large increase of a broad spectrum of $m = 1$ modes, with a consequent deterioration of plasma confinement, generates a large dynamo electric $E_{d,\phi} \simeq 15$ V/m [7]. In QSH plasmas, however, a significant continuous dynamo driven primarily by one dominant mode appears between these discrete MH events, in contrast to very weak continuous multimode dynamo present between sawtooth crashes in fully MH plasmas. Even if the present QSH regime does not produce a fully efficient dynamo, since MH discrete dynamo events are still present, these results are important as a proof of principle, since they show that a more continuous and less turbulent dynamo can exist away from discrete dynamo events in RFP plasmas.

[1] D. Biskamp, *Magnetohydrodynamic Turbulence* (Cambridge University Press, Cambridge, 2003).
[2] A. Gailitis *et al.*, Phys. Rev. Lett. **86**, 3024 (2001).
[3] H. Ji and S. C. Prager, Magnetohydrodynamics **38**, 191 (2002).
[4] W. X. Ding *et al.*, Phys. Rev. Lett. **93**, 045002 (2004).
[5] S. Ortolani and D. D. Schnack, *Magnetohydrodynamics of Plasma Relaxation* (World Scientific, Singapore, 1993).
[6] P. Martin *et al.*, Nucl. Fusion **42**, 247 (2002).
[7] D. J. Den Hartog *et al.*, Phys. Plasmas **6**, 1813 (1999).
[8] P. W. Fontana *et al.*, Phys. Rev. Lett. **85**, 566 (2000).
[9] S. Cappello and D. Biskamp, Nucl. Fusion **36**, 571 (1996).
[10] G. Fiksel *et al.*, Phys. Rev. Lett. **72**, 1028 (1994).
[11] T. M. Biewer *et al.*, Phys. Rev. Lett. **91**, 045004 (2003).
[12] S. Cappello and D. F. Escande, Phys. Rev. Lett. **85**, 3838 (2000).
[13] D. F. Escande *et al.*, Phys. Rev. Lett. **85**, 3169 (2000).
[14] D. F. Escande *et al.*, Phys. Rev. Lett. **85**, 1662 (2000).
[15] L. Marrelli *et al.*, Phys. Plasmas **9**, 2868 (2002).
[16] R. A. Nebel *et al.*, Phys. Fluids B **1**, 1671 (1989).
[17] J. M. Finn *et al.*, Phys. Fluids B **4**, 1292 (1992).
[18] R. N. Dexter *et al.*, Fusion Technol. **19**, 131 (1991).
[19] D. J. Den Hartog and R. J. Fonck, Rev. Sci. Instrum. **65**, 3238 (1994).
[20] J. T. Chapman, Ph.D. thesis, University of Wisconsin, Madison, 1998.
[21] V. Antoni and S. Ortolani, Plasma Phys. Controlled Nucl. Fusion Res. **25**, 799 (1983).
[22] W. X. Ding *et al.*, Phys. Rev. Lett. **90**, 035002 (2003).
[23] J. S. Bendat and A. G. Piersol, *Random Data* (Wiley, New York, 2000).